Design, synthesis and neuroprotective evaluation of novel tacrine–benzothiazole hybrids as multi-targeted compounds against Alzheimer's disease

Rangappa S. Keri [a], Catarina Quintanova [a], Sérgio M. Marques [a], A. Raquel Esteves [b], Sandra M. Cardoso [b,c], M. Amélia Santos [a,*]

[a] Centro de Quimica Estrutural, Instituto Superior Técnico, Universidade Técnica de Lisboa, Av. Rovisco Pais 1, 1049-001 Lisboa, Portugal
[b] Centro de Neurociencias e Biologia Celular, Universidade de Coimbra, 3030 Coimbra, Portugal
[c] Faculdade de Medicina, Universidade de Coimbra, 3030 Coimbra, Portugal

ABSTRACT

Alzheimer's disease (AD) is a multifactorial disorder with several target proteins contributing to its etiology. In search for multifunctional anti-AD drug candidates, taking into account that the acetylcholinesterase (AChE) and beta-amyloid (Aβ) aggregation are particularly important targets for inhibition, the tacrine and benzothiazole (BTA) moieties were conjugated with suitable linkers in a novel series of hybrids. The designed compounds (**7a**–**7e**) were synthesized and in vitro as well as in ex vivo evaluated for their capacity for the inhibition of acetylcholinesterase (AChE) and Aβ self-induced aggregation, and also for the protection of neuronal cells death (SHSY-5Y cells, AD and MCI cybrids). All the tacrine–BTA hybrids displayed high in vitro activities, namely with IC_{50} values in the low micromolar to sub-micromolar concentration range towards the inhibition of AChE, and high percentages of inhibition of the self-induced Aβ aggregation. Among them, compound **7a**, with the shortest linker, presented the best inhibitory activity of AChE ($IC_{50} = 0.34 \mu M$), while the highest activity as anti-Aβ42 self-aggregation, was evidenced for compound **7b** (61.3%, at 50 μM. The docking studies demonstrated that all compounds are able to interact with both catalytic active site (CAS) and peripheral anionic site (PAS) of AChE. Our results show that compounds **7d** and **7e** improved cell viability in cells treated with Aβ42 peptide. Overall, these multi-targeted hybrid compounds appear as promising lead compounds for the treatment of Alzheimer's disease.

© 2013 Elsevier Ltd. All rights reserved.

1. Introduction

Neurological disorders inflict a heavy burden on healthcare costs, affecting individuals and their caregivers. Alzheimer's disease (AD) is classified as a progressive, neurodegenerative disease that affects the cholinergic regions of the central nervous system (CNS) that associates with cognitive function and spatial awareness.[1] Data of 2010 reported that it affected approximately 36 million people worldwide, being expected to increase up to 114 million by 2050.[2] The etiopathogenesis of this multifactorial disease still remains unknown, although, in the last decades, several involved factors have been identified and found consistent with its onset. Among them is the impairment of the cholinergic system, as indicated by the presence of altered cholinergic markers in AD patients, resulting in a pronounced acetylcholine (ACh) deficiency which translates into a generalized cognitive decline.[3,4] Other hallmarks of AD patient brains is the misfolding and aggregation of specific proteins that accumulate intracellularly (e.g., neurofibrillary tangles,[5,6] containing hyperphosphorylated tau protein) or extracellularly (e.g., senile plaques,[7,8] mostly composed of beta-amyloid peptide (Aβ) aggregates) that interfere with relevant brain biological functions.

There have been many approaches to potential therapies, but to date cholinesterase inhibitors (ChEIs) were the first and the only class of drugs in the market that showed some results in the treatment of AD. Tacrine, donepezil, rivastigmine and galantamine (Fig. 1) are examples of acetylcholinesterase (AChE) inhibitors that have been approved by the US Food and Drug Administration (FDA). These inhibitors have beneficial effects on cognitive, functional and behavioral symptoms of AD.[9,10]
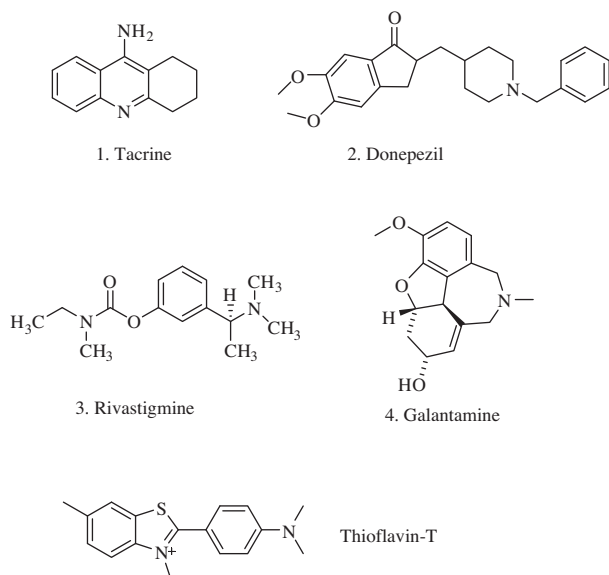
Figure 1. Chemical structure of reported AChE inhibitors (tacrine, donepezil, rivastigmine and galantamine), and an Aβ-aggregation inhibitor (thioflavin-T).

Figure 2. Design strategy for the new series of tacrine–benzothiazole hybrids.

Among them, tacrine was the first AChE inhibitor approved by the FDA for the treatment of AD.[11,12] Recent studies have demonstrated that homo- and hetero-dimers can improve the biological profile of tacrine and even overcome some of its side effects.[13] Afterwards, quite a number of tacrine derivatives, some of them as hybrid potential drugs, have been developed to improve its activity, as described in a recent review in this topic,[14] including tacrine–8-hydroxyquinoline,[15] mercapto-tacrine derivatives,[16] tacrine–fluorobenzoic acid[17] and tacrine–multialkoxybenzene hybrids.[18]

Moreover, based on evidences that reduction of amyloid deposits lead to alleviation of the AD's symptoms,[19,20] a considerable current effort has been directed towards the identification and the development of potential therapeutic agents able to reduce the soluble amyloid oligomers burden.[21,22] Among the many compounds known for strongly interacting with the Aβ peptides, some include the benzothiazole (BTA) moiety in the main scaffold (e.g., the dye thioflavin-T (ThT, Fig. 1)).[23] Thus, some BTA derivatives have been used as Alzheimer's brain imaging agents,[24] while others have evidenced capacity for inhibiting the peptide aggregation and neuro-protective roles.[25,26]

More recently quite a number of studies have been focused on the development of therapeutic strategies multitarget drugs to fight multifactorial neurodegenerative disorders, such as AD. Thus, one of the most explored design strategies has been focused on the development of hybrids that combine the ChEs inhibition role, for the enhancement of the cholinergic neurotransmission, with other relevant roles (e.g., reduction the Aβ fibril self-aggregation, antioxidant and metal depletion).[27–30] In this context, the development of tacrine–BTA hybrid compounds appears as important challenge, because they could be expected not only to act in the symptomatic effects but also in the underlying molecular etiology of the disease.[22] Therefore, we have designed a series of novel multifunctional compounds by conjugating a tacrine and a BTA moiety through different suitable linkers. A selection of these compounds (Figs. 2 and 3) was synthesized and evaluated for their in vitro activity as inhibitors of AChE and of self-induced Aβ aggregation, as well as for their antioxidant activity, because oxidative stress is thought to play a major role in the pathogenesis of AD.[31] In order to evaluate the biological neuroprotective role of these compounds, we determined their effect on the cell viability using different AD cellular models exposed to Aβ peptides.
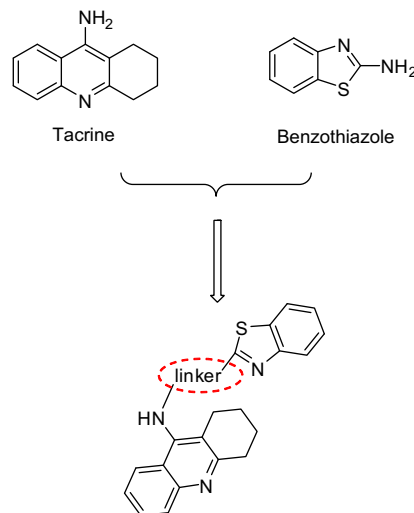
2. Results and discussion

2.1. Molecular modeling

The strategy followed for the design of the new inhibitors consisted of making a pre-selection of several connecting groups (spacers) between the two main moieties, the tacrine and the BTA (Fig. 1), and then performing the virtual screening of these molecules against a target enzyme (AChE) involved in the cholinergic loss. The active site of this molecule is found in a deep pocket were acetylcholine (substrate) can slip inside and be hydrolyzed into acetic acid and choline, which is no longer a neurotransmitter. At the base of the pocket there is the catalytic triad, composed of Ser200, His440 and Glu327. Within the pocket of AChE there is also the catalytic active site (CAS), which is formed by two important amino acids, the Phe330 and Trp84. The AChE also contain a peripheral active site (PAS), which is located at the entrance of the gorge and is formed by Trp279 and Tyr70 (sequence numbering of Torpedo californica AChE, TcAChE).

The docking study was carried out using program GOLD, v. 5.1.[32] The crystal structure of TcAChE complexed with an inhibitor was taken from RCSB Protein Data Bank (PDB, entry 1ODC).[33] This structure was chosen because of the similarity between its inhibitor and the synthesized ligands. The original ligand (N-quinolin-4-yl-N′-(1,2,3,4-tetrahydroacridin-9-yl)octane-1,8-diamine) is formed by tacrine connected through a long carbon chain to an aminoquinoline moiety, which is structurally very similar to the BTA moiety. The docking calculations were performed using the ASP scoring function, since this function has previously proven to give the best docking predictions for AChE inhibitors.[30,34]

The docking studies revealed favorable interactions for the new inhibitors (see Fig. 3), with many similarities in their binding conformations. In Fig. 4 are displayed the main docking results. These show the ligands well inserted into the cavity of the active site blocking the entrance to the substrate (choline) and water molecules. The tacrine moiety is always found well inserted in the bottom of the gorge of the enzyme, binding to the CAS by π–π stack with the aromatic ring of Trp84 and Phe330, overlapping almost perfectly with the tacrine moiety of the original ligand (see Fig. S1, Supplementary data). Generally, the spacer seems to be well accommodated along the hydrophobic cavity. On the other hand, the BTA moiety was always placed at the entrance of the gorge, and, except for **7b**, it is able to bind to PAS forming aromatic stacking with Tyr70 and Trp279. For **7b** (Fig. 4a) it is the phenyl
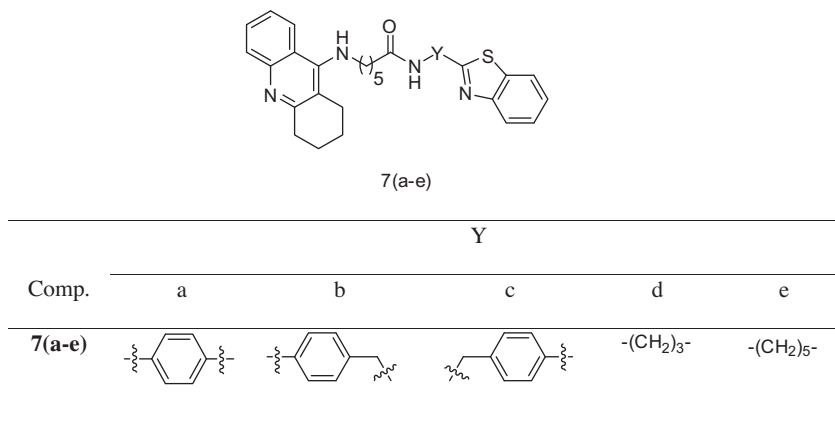
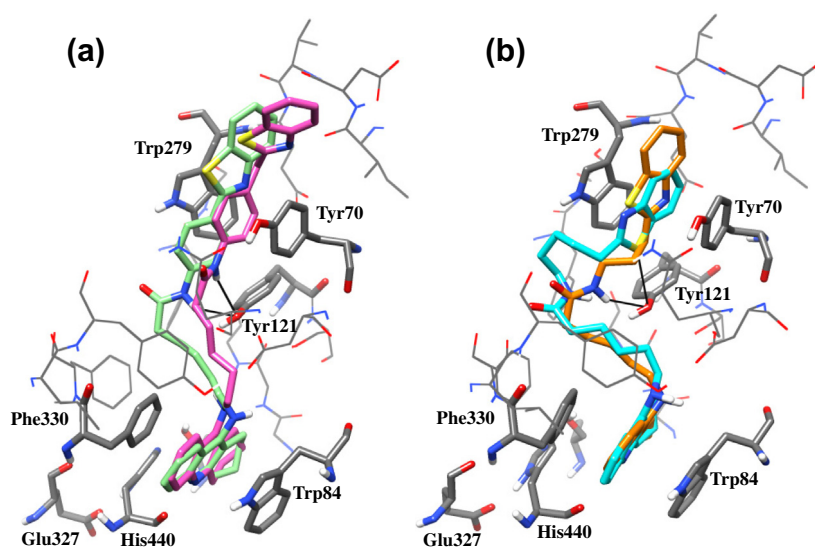Figure 3. Synthesized tacrine–BTA hybrid compounds.

Figure 4. Docking results for the tacrine–BTA hybrids with AChE: superimposition of **7a** (light green) with **7b** (pink) (a), and **7d** (orange) with **7e** (cyan) (b). H-bonds are represented as solid black lines.

ring of the spacer that forms such aromatic interaction with Tyr70 and Trp279, thus allowing maintaining the strong interactions with the enzyme. Moreover, a favorable H-bond formed between the amide NH group of the linker with Tyr121 OH group in the cases of **7a** and **7b**, which cannot be formed with **7c**, explains the lower inhibitory capacity of the last compound compared to the first two (Fig. 4a and Fig. S2). Regarding compounds **7d** and **7e** (Fig. 4b), the BTA is in position to performs the same aromatic interaction with PAS. The possibility of the Tyr121 OH group to form H-bond with both of these ligands, either through the amide NH group (**7d**) or the sulfur atom of the BTA (**7e**) allows the inhibitory activity to increase, with regards to **7c**, up to sub-micromolar values. Considering the vicinity of the NH group of the linker in **7e** with the Tyr121 OH group (Fig. 4b), we may expect that this residue can dynamically alternate the H-bonding between the BTA sulfur atom and that NH group. This fact would explain the higher activity of **7e** compared to **7d** (see below).

Globally, these modeling studies foresee the ability of the compounds to interact with both the CAS and PAS, and the features disclosed allow explaining the good inhibitory activities observed with AChE (Table 1). Several studies have pointed out the role of AChE in the Aβ fibrils formation, and that compounds interacting with PAS may have an inhibitory effect in Aβ aggregation.[35,36]

Therefore, we may expect that this new family of hybrid compounds also prevent this type of amyloid fibrillation.

2.2. Chemistry

The tacrine–benzothiazole hybrids (**7a–7e**) were synthesized as shown in Scheme 1. The 9-chloro-1,2,3,4-tetrahydroacridine (**3**) was prepared from commercially available anthranilic acid, as previously reported.[37,38] Compound **3** was treated with 6-amino-hexanoic acid, using a catalytic amount of KI and phenol, to give the 2-(1,2,3,4-tetrahydroacridine-9-ylamino) acid (**5**). Finally, the carboxylic group of this compound (**5**) was condensed with a series of different amino-benzothiazole derivatives (**6**) with formation of amide linkages, using 1-(3-dimethylaminopropyl)-3-ethylcarbodiimide hydrochloride (EDCI·HCl) and 4-dimethylaminopyridine (DMAP), affording the tacrine–BTA hybrid compounds (**7**).

2.3. Biological activity

2.3.1. AChE inhibition

The enzymatic activities of the newly synthesized compounds **7**(**a**–**e**) were evaluated by adaptation of the spectroscopic method described by Ellman.[30] The IC$_{50}$ values for AChE inhibition are

Table 1
In vitro activities of the tacrine–BTA derivatives towards AChE inhibition, Aβ aggregation and antioxidant activity (DPPH assay)
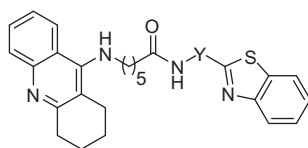
7(a-e)

| S. No.	Compd code	Y	AChE inhibitor IC$_{50}$[a] (μM)	Aβ aggregation inhibition[b,c]	Antioxidant activity[d] (μM)
1	**7a**	–Ph–	0.34 ± 0.1	22.3	32% (1.32 mM)
2	**7b**	–PhCH$_2$–	0.57 ± 0.1	61.3	>1000
3	**7c**	–CH$_2$Ph–	1.84 ± 0.2	29.9	>1000
4	**7d**	–(CH$_2$)$_3$–	0.96 ± 0.3	35.0	25% (1.22 mM)
5	**7e**	–(CH$_2$)$_5$–	0.76 ± 0.4	22.3	>1000
6	Tacrine	–	0.19 ± 0.04	n.d.[e]	>1000

[a] The values are mean of three independent experiments ± SD.
[b] Inhibition of self-mediated Aβ$_{42}$ aggregation (in %). The thioflavin-T fluorescence method was used, and the measurements were carried out in the presence of inhibitor (50 μM).
[c] The values are the mean of two independent measurements in duplicate (SEM < 10%).
[d] EC$_{50}$ values for the DPPH assay, or the % of quenching for the concentration in brackets.
[e] Not determined.
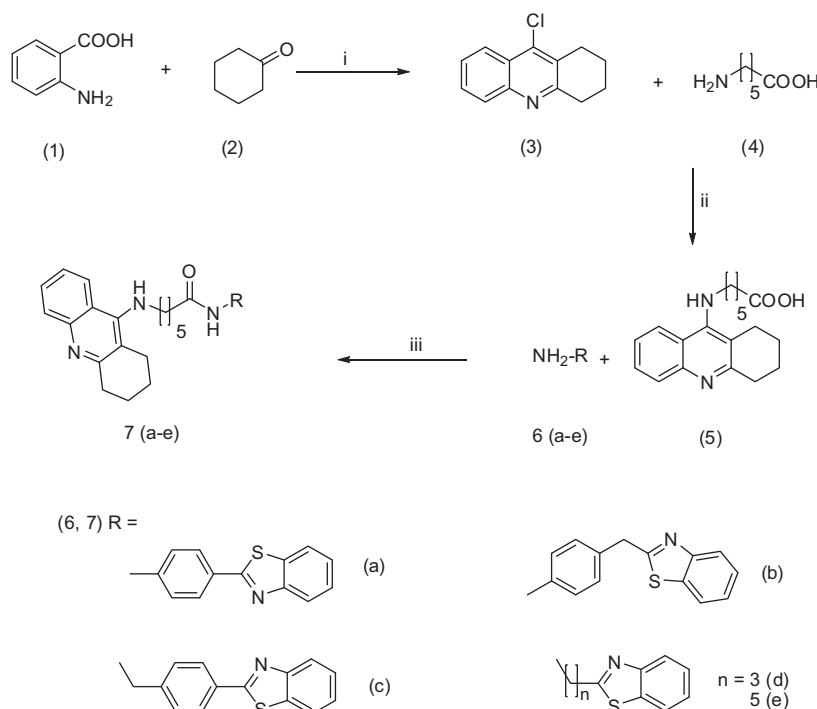
Scheme 1. Synthesis of the tacrine–BTA hybrids **7**(**a–e**). Reagents and conditions: (i) POCl$_3$, 3 h, 180 °C; (ii) phenol, KI, 4 h, 180 °C; (iii) DCM, EDCI·HCl DMAP, 24 h, rt.

summarized in Table 1. As expected, all the tacrine–BTA hybrids displayed high inhibitory activities against this enzyme, with IC$_{50}$ values in the sub-micromolar to low micromolar range. Although the new compounds have less capability to inhibit the enzyme when compared to the reference drug, tacrine, some of them presented activities with the same order of magnitude (sub-micromolar). Among these, **7a** appears to be the strongest inhibitor, with IC$_{50}$ value of 0.34 μM, quite similar to that obtained for tacrine (IC$_{50}$ = 0.19 μM), followed by **7b** with 0.51 μM. The compound with the weakest inhibitory activity is **7c**, with IC$_{50}$ value of 1.84 μM. A structure–activity relationship analysis shows that the inhibitory potency against AChE is closely related with the length of the

linker, as well as its composition and geometry. Analysis of the results suggests that a five carbon linker seems to provide a suitable length between the tacrine and the connecting amide bond. On the other hand, the aromaticity and geometry of the Y spacer near the BTA group appears to have a relevant role in this enzymatic activity. In fact, the presence of a simple phenyl group attached to the BTA moiety, as in **7a**, IC$_{50}$ = 0.34 μM), endowed the highest inhibition capacity. The introduction of a methylene group (and a concomitant angle) between the phenyl ring and the BTA, as in **7b**, resulted in small activity reduction (IC$_{50}$ = 0.51 μM), whereas the identical insertion, but between the amide bond and the Ph–BTA moiety, resulted in a considerable activity reduction (**7c**,

1.84 μM). On the other hand, when a linear aliphatic Y spacer is introduce, there is a retrieval in the inhibitory capacity (**7d**–**e**), which is more pronounced with a longer and more flexible five-carbon chain (**7e**, 0.76 μM). These observations are in good agreement with the results obtained from the docking studies (see above). The fact that the new compounds are weaker inhibitors than tacrine suggests some associated weakening of their binding interactions with the enzyme. However, as dual binding-site inhibitors, it is expected that the BTA group can bind the peripheral anionic site (PAS) of AChE. According to reported evidences,[35] this feature is expected to reduce the cholinergic-induced aggregation of the Aβ peptide, and thus enhance the overall anti-Aβ aggregation ability of these multifunctional hybrid compounds.

2.3.2. Inhibition of self-mediated Aβ₄₂ aggregation

To test the anti-amyloidogenic activity of the new compounds, our experimental approach relies on in vitro assays with ThT to monitor and quantify the aggregation of Aβ₄₂ synthetic peptide into fibrils. ThT is a histochemical dye that is known to bind to the peptide β-sheet conformation, which is the predominant secondary structure of amyloid-beta fibrils. The presence of fibrils can be monitored by the fluorescence emission of ThT, with the absorption peak at 446 nm and the emission peak at 490 nm.[39–41] The inhibition studies were carried out upon incubating Aβ₄₂ with and without the compounds. The results (summarized in Table 1) show that all the compounds induced a decrease of the ThT fluorescence associated with the Aβ fibril binding, thus indicating an inhibition of the Aβ₄₂ self-aggregation process. In particular, all of them presented aggregation inhibition values above 20% (in a concentration ratio of 1:2.5 [Aβ:I]), whereas **7b** presented the best activity (61.3%). This could be explained by the conformation adopted by this compound in solution, which may allow the best interaction of the BTA moiety with β-sheet secondary structure of Aβ peptides. Therefore it can be hypothesized that a BTA-moiety composed of a biaryl heterocyclic scaffold is better able to recognize and interact with the abnormal β-sheet conformation of the Aβ peptide, and to endow the inhibition of the fibrilogenesis.

2.3.3. In vitro neuroprotective activity

To evaluate the potential therapeutic action of tacrine–benzothiazole hybrid compounds, SHSY-5Y cells, AD, MCI (mild cognitive impairment) and control cybrids were treated with Aβ₄₂ peptides. In fact, Aβ₄₂ treatments in human cell lines constitute a reliable model for screening potential neuroprotective compounds because they mimic some aspects of neurodegeneration underlying the AD physiopathology. Moreover, since AD and MCI cybrids perpetuate the defects found in the brains and peripheral tissues, it is reasonable to argue that the screening of new disease-modifying drugs in these ex vivo cellular models could give valuable information. In addition, the use of MCI cybrids, that harbor MCI individuals mitochondria allowed us to target an early phase of the disease development.[42] An early identification of individuals in the preclinical period that are not yet demented is imperative, in order to potentiate the effect of disease-modifying agents.[43]

Our results (see Fig. 5) evidenced a significant protection of some compounds, namely **7d** and **7e**, on Aβ₄₂ induced toxicity in SHSY-5Y cells and in MCI and AD cybrids. However, we did not see the same for control cybrids where only compound **7a** prevented Aβ₄₂ toxicity. Our results highlight the importance of multi-targeted anti-neurodegenative drugs, like tacrine–BTA hybrids that act as inhibitors of AChE and Aβ oligomerization, on the prevention of Aβ₄₂ peptides-induced toxicity. By using different cellular models mimicking AD (AD cybrids) and targeting the intermediate state between normal aging and AD (MCI cybrids)

we showed that these new set of hybrid tacrine–BTA compounds have relevant protective properties that may act as candidate molecules to prevent or arrest AD pathology.

2.3.4. Antioxidant activity

The new compounds were screened for their anti-oxidant activities (EC₅₀), based on their interaction with the 2,2-diphenyl-1-picrylhydrazyl (DPPH) free radical,[44] and the corresponding results are summarized on Table 1. Analysis of the results clearly shows that, as expected, none of new compounds exhibits significant antioxidant activities, as it is shown by the low inhibition percentages at very high concentrations (25–32% at millimolar concentration). The insignificant radical-capture capacity of the tested compounds can be explained by the absence of phenolic hydroxyl groups that are important in the scavenging action of ROS species. Tacrine moiety is present in all the compounds, and tacrine alone has no significant antioxidant activity. Since there are no extra-functional groups in compounds **7a**–**7e** capable of reducing the DPPH radical, similar results were expected for the new compounds.

2.3.5. Pharmacokinetic properties

In order to estimate the potential of the new compounds as eventual drugs, a few indicators of their pharmacokinetic profiles were predicted using QikProp program, v. 2.5.[45] Parameters such as the calculated lipo-hydrophilic character (clogP), the ability to cross the blood–brain barrier (log BB), their ability to be absorbed through the intestinal tract to the blood (Caco-2 cell permeability), and the verification of *Lipinski's rule of five*, may give an idea of their *druglikeness* for being orally used as anti-AD agents.

As observed in Table 2, all the compounds presented clogP (octanol/water) coefficients superior to five, while **7a** and **7b** are even greater than 6.5. This fact leads this set of compounds to have a lipophilic character higher than recommended by *Lipinski's rule*.[46] The compounds also have molecular weights higher than 500, which accounts for two violations of this rule, except for compound **7d**, which seems to present better results within this set of compounds.

The high lipophilic character and the low blood–brain barrier permeability (log BB) indicate that the compounds are not eligible drug candidates for oral administration, and further improvement will be necessary to ameliorate compound absorption and entering into the cells. However, they exhibited very good results in Caco-2 permeability, ranging from ca. 1000 to 2000 nm/s (higher than 500 nm/s is considered good[45]), indicating that the absorption through the intestinal tract to the blood is possible.

3. Conclusions

Taking into account the multifactorial processes involved in Alzheimer's disease, the development of drugs that could modulate multiple targets simultaneously with eventual synergistic effects seems to be the wisest strategy for improving drug efficacy. In the present study a set of bi-targeting compounds, based on tacrine were designed and their protective action, as potential anti-neurodegenerative drugs, was investigated. Specifically a novel family of tacrine–BTA hybrids has been assessed for the AChE inhibition, Aβ self-induced aggregation, antioxidant properties and also protective roles in cellular models mimicking AD. Our results showed that four compounds had high cholinesterase inhibitory activities with IC₅₀ values bellow 1 μM against AChE. Among them, compound **7a** showed good AChE activity (IC₅₀ = 0.34 μM), similarly to the commercial drug tacrine (0.19 μM). The length, geometry and aromaticity of the Y spacer (nearby the BTA moiety) revealed determinant for the activity. All the synthesized compounds were
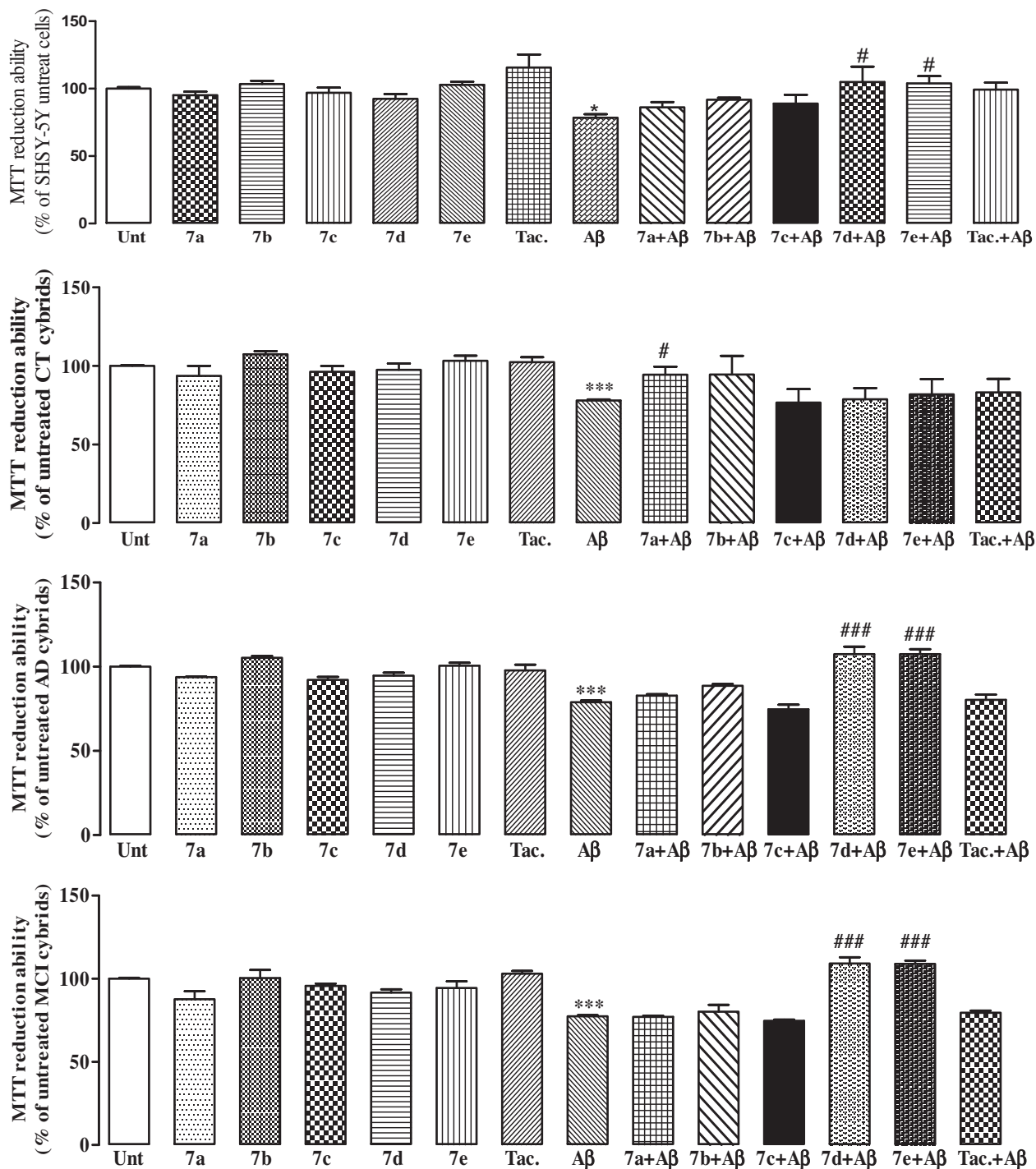
Figure 5. Effect of tacrine–BTA hybrids on $A\beta_{42}$- induced toxicity in AD cellular models. Cells were treated with $Abeta_{1-42}$ (1 μM) peptides, for 24 h, in the absence or the presence of 2.5 μM of compounds **7a–e** or tacrine. Evaluation of cell viability was performed by using MTT reduction test. Results are expressed as the percentage of untreated cells, with the mean ± SEM derived from 3 different experiments. $^*p < 0.05$; $^{***}p < 0.001$, significantly different when compared with untreated cells; $^\#p < 0,05$; $^{\#\#\#}p < 0,001$, significantly different when compared with $A\beta_{42}$ treated cells.

capable of inhibiting $A\beta_{42}$ self-aggregation process (above 20% at a 50 μM of inhibitor), and **7b** showed the best value with 61.3% of aggregation inhibition. All the compounds showed low antioxidant activity (ca. 25–30% for ca. 1 mM towards DPPH). Molecular modeling studies of the AChE-inhibitor interaction allowed the rationalization of the SAR observed. They confirmed that these hybrid inhibitors target both the catalytic active site (CAS) and peripheral anionic site (PAS) of AChE, highlighting their potential to also inhibit the cholinergic-induced $A\beta$ aggregation.

Our cellular studies demonstrated that some of these compounds, in particular **7d** and **7e**, provided substantial protection from cell death (SHSY-5Y cells, AD and MCI cybrids) induced by $A\beta_{42}$ peptides, a reliable model for screening potential neuroprotective roles.

Overall, our preliminary findings showed that this new set of hybrid tacrine–BTA compounds can merge important properties, such as AChE inhibition and interaction with $A\beta$. Hence, they are able to act on one of the leading events of AD and on one of AD

Table 2
Predicted pharmacokinetic values

S. No.	Compd code	Y	$c \log P$ [a,b]	log BB [a,c]	Caco -2 permeability[a] (nm/s)	Violations of Lipinski's rule of 5[a]
1	**7a**	Ph	6.61	−0.59	2028	2
2	**7b**	CH$_2$Ph	7.44	−1.06	1436	2
3	**7c**	PhCH$_2$	5.37	−0.35	2271	2
4	**7d**	(CH$_2$)$_3$	5.23	−0.64	1389	1
5	**7e**	(CH$_2$)$_5$	5.14	−0.75	1044	2
6	Tacrine	–	2.53	0.04	2880	0

[a] Predicted values using program QikProp v. 2.5.[45]
[b] Calculated octanol/water partition coefficient.
[c] Brain/blood partition coefficient.

pathological hallmark, revealing as potential lead compounds towards AD therapy.

4. Experimental part

4.1. Chemistry

4.1.1. General methods and materials

Analytical grade reagents were purchased from Sigma–Aldrich, Fluka and Acros and were used as supplied. Solvents were dried according to standard methods.[47] The chemical reactions were monitored by TLC using alumina plates coated with silica gel 60 F$_{254}$ (Merck). Column chromatography separations were performed on silica gel Merck 230–400 mesh (Geduran Si 60). The melting points were measured with a Leica Galen III hot stage apparatus and are uncorrected. The ^{1}H and ^{13}C NMR spectra were recorded on Bruker AVANCE III spectrometers at 300 MHz and 400 MHz, respectively. Chemical shifts (δ) are reported in ppm from the standard internal reference tetramethylsilane (TMS). The following abbreviations are used: s = singlet, d = doublet, t = triplet, m = multiplet. Mass spectra (ESI-MS) were performed on a 500 MS LC Ion Trap (Varian Inc., Palo Alto, CA, USA) mass spectrometer equipped with an ESI ion source, operated in the positive ion mode. For the target compounds, the elemental analyses were performed on a Fisons EA1108 CHNS/O instrument and were within the limit of ±0.4%.

4.1.2. 9-Chloro-1,2,3,4-tetrahydroacridine (3)

To a mixture of anthranilic acid (3.2 g, 23 mmol) and cyclohexanone (2.65 mL, 27 mmol) in an ice bath, POCl$_3$ (25 mL) was carefully added. The mixture was heated under reflux for 3 h, then cooled at room temperature, and concentrated to give slurry. The residue was diluted with EtOAc, neutralized with aqueous K$_2$CO$_3$, and washed with brine. The organic layer was dried over anhydrous K$_2$CO$_3$ and concentrated in vacuo, affording a pale brown solid. It was recrystallized from acetone to give **3** (4.6 g, 91%). Mp 67–69 °C (lit. mp 66–68 °C);[48] ^{1}H NMR (300 MHz, CDCl$_3$) δ: 8.16 (d, J = 7.5 Hz, 1H, ArH), 7.97 (d, J = 8.3 Hz, 1H, ArH), 7.65 (dd, J = 9.2, 7.5 Hz, 1H, ArH), 7.52 (t, J = 8.3 Hz, 1H, ArH), 3.10 (t, J = 6.3 Hz, 2H, CH_2), 3.01 (t, J = 4.8 Hz, 2H, CH_2), 1.94 (br s, 4H, CH_2–CH_2); m/z: 218 (M$^+$), 219 (M+1)$^+$, 220 (M+2)$^+$.

4.1.3. 2-(1,2,3,4-Tetrahydroacridine-9-ylamino)acetic acid (5)

To a mixture of 9-chloro-1,2,3,4-tetrahydroacridine (3.18 g, 1.46 mmol) and 6-amino-hexanoic acid (3.83 g, 2.92 mmol) was added phenol (1.5 g) and catalytic amount of KI (50 mg). The mixture was heated at 180 °C for 4 h and then cooled to room temperature. The mixture was dissolved in 5% NaOH, washed with diethyl ether (3–4 times). The collected aqueous layer was adjusted to pH 8 with HCl (concd), then, once again, washed with diethyl ether

(3–4 times). The aqueous layer was acidified with HCl (concd) up to pH 2 and then extracted with dichloromethane. The organic layer was dried over anhydrous Na$_2$SO$_4$ and concentrated in vacuo to give the pure compound as pale yellow oil (2.73 mg). Yield: 60%; ^{1}H NMR (300 MHz, MeOD) δ: 8.37 (d, J = 8.3 Hz, 1H, ArH), 7.97–7.83 (m, 2H, ArH), 7.60–7.55 (m, 1H, ArH), 3.95 (t, J = 7.3 Hz, 2H, CH_2), 3.02 (s, 2H, CH_2), 2.70 (s, 2H, CH_2), 2.30 (t, J = 7.20 Hz, 2H, CH_2), 1.96 (br s, 4H, CH_2–CH_2), 1.85 (t, J = 7.20 Hz, 2H, CH_2), 1.62 (t, J = 7.60 Hz, 2H, CH_2), 1.51–1.43 (m, 2H, CH_2); ^{13}C NMR (400 MHz, CDCl$_3$) δ: 178.7 (C=O), 156.1, 150.3, 138.3, 132.7, 125.8, 125.6, 119.1, 115.7, 111.7 (9 aromatic C), 51.2 (N-CH$_2$ aliphatic chain), 48.1, 34.2, 30.6, 28.6, 26.1, 24.4, 22.0, 20.8 (9 aliphatic C); m/z: 313 (M$^+$), 314 (M+1)$^+$.

4.1.4. General procedure for the synthesis of the benzothiazole derivatives 6(a–e)

A mixture of 2-aminothiophenol (1 equiv) and different substituted amino-carboxylic acids (4-aminobenzoic acid, 4-aminophenylacetic acid, 4-(aminomethyl)benzoic acid, 4-aminobutyric acid and 4-aminohexanoic acid) (1 equiv) in polyphosphoric acid (15 g) was stirred at 220 °C for 4 h. The resulting brown oil was dissolved in 5 M NaOH (50 mL) to obtain basic yellow solution and this solution was extracted with DCM (2 × 30 mL). The total organic phase was then extracted with 0.1 N HCl (2 × 30 mL) and afterwards washed DCM (50 mL). The aqueous phase was basified to pH ~10–12 with 5 M NaOH, and it was extracted with DCM (2 × 30 mL). The total organic phase was dried over anhydrous Na$_2$SO$_4$, and the solvent evaporated. The brown oil obtained was treated with HCl-saturated methanol until pH ~1, the solution was evaporated, and the residue was recrystallized from acetonitrile.

4.1.4.1. 4-(Benzo[d]thiazol-2-yl)aniline (6a). 2-Aminothiophenol and 4-aminobenzoic acid afforded the pure title product as a greenwish solid.[49] Yield: 64%; ^{1}H NMR (300 MHz, MeOD) δ: 7.80 (d, J = 8.8 Hz, 2H, NC-CH and SC-CH), 7.47 (d, J = 8.9 Hz, 2H, CH-CHNH$_2$), 7.42 (t, J = 8.9 Hz, 1H, NC-CHCH), 7.30 (t, J = 8.9 Hz, 1H, SC-CHCH), 6.75 (d, J = 9 Hz, 2H, CH-CHNH$_2$). m/z (ESI) 227.1 (M+H)$^+$.

4.1.4.2. 4-(Benzo[d]thiazol-2-ylmethyl)aniline (6b). 2-Aminothiophenol and 4-aminophenylacetic acid afforded the pure title product as a brown solid.[30] Yield: 62%; ^{1}H NMR (300 MHz, MeOD) δ: 7.95 (d, J = 8.9 Hz, 1H, NC-CH), 7.88 (d, J = 9 Hz, 1H, SC-CH), 7.60 (d, J = 8.8 Hz, 2H, CH-CHNH$_2$), 7.48 (t, J = 9 Hz, 2H, NC-CHCH, SC-CHCH), 7.42 (d, J = 9 Hz, 2H, CHCH-NH$_2$), 4.41 (s, 2H, CH_2). m/z (ESI) 241.1 (M+H)$^+$.

4.1.4.3. (4-(Benzo[d]thiazol-2-yl)phenyl)methanamine (6c). 2-Aminothiophenol and 4-(aminomethyl)benzoic acid afforded the pure title product as a yellow solid.[30] Yield: 68%; ^{1}H NMR (300 MHz, MeOD) δ: 8.20 (d, J = 8 Hz, 2H, NC-CH and SC-CH), 8.09 (d, J = 8.9 Hz, 2H, HC-CHCH$_2$NH$_2$), 7.60 (d, J = 9 Hz, 2H, HC-CH$_2$NH$_2$), 7.58 (t, J = 7.8 Hz, 1H, NC-CHCH), 7.51 (t, J = 9 Hz, 1H, SC-CHCH), 4.24 (s, 2H, CH_2). m/z (ESI) 241.1 (M+H)$^+$.

4.1.4.4. 3-(Benzo[d]thiazol-2-yl)propan-1-amine (6d). 2-Aminothiophenol and 4-aminobutyric acid afforded the pure title product as a brown solid. Yield: 69%; ^{1}H NMR (300 MHz, D$_2$O) δ: 7.90 (d, J = 7.9 Hz, 1H, NC-CH), 7.83 (d, J = 8 Hz, 1H, SC-CH), 7.53 (t, J = 7.2 Hz, 1H, NC-CHCH), 7.47 (1H, t, J = 7.2 Hz, SC-CHCH), 3.22 (t, J = 7.6 Hz, 2H, H$_2$N(CH$_2$)$_2$CH_2), 3.11 (t, J = 7.7 Hz, 2H, H$_2$NCH_2(CH$_2$)$_2$), 2.26–2.04 (m, 2H, H$_2$NCH$_2$CH_2CH$_2$). m/z (ESI) 193.0 (M+H)$^+$.

4.1.4.5. 5-(Benzo[*d*]thiazol-2-yl)pentan-1-amine (6e).

2-Aminothiophenol and 4-aminohexanoic acid afforded the pure title product as a brown solid. Yield: 75%; ^{1}H NMR (300 MHz, D$_2$O) δ: 7.98 (d, *J* = 8.0 Hz, 1H, NC-C*H*), 7.86 (d, *J* = 8 Hz, 1H, SC-C*H*), 7.57 (t, *J* = 7.0 Hz, 1H, NC-CHC*H*), 7.50 (t, *J* = 7.2 Hz, 1H, SC-CHC*H*), 3.19 (t, *J* = 7.7 Hz, 2H, N(CH$_2$)$_4$C*H*$_2$), 2.99 (t, *J* = 7.6 Hz, 2H, H$_2$NC*H*$_2$(CH$_2$)$_4$), 1.93–1.83 (m, 2H, H$_2$N(CH$_2$)$_3$C*H*$_2$CH$_2$), 1.77–1.67 (m, 2H, H$_2$NCH$_2$C*H*$_2$(CH$_2$)$_3$), 1.52–1.42 (m, 2H, H$_2$N(CH$_2$)$_2$C*H*$_2$(CH$_2$)$_2$). *m/z* (ESI) 193.0 (M+H)$^+$.

4.1.5. General procedure for the synthesis of the tacrine–benzothiazole compounds (7a–e)

1-(3-Dimethylaminopropyl)-3-ethylcarbodiimide hydrochloride (EDCI·HCl) (2.5 equiv) and 4-dimethylaminopyridine (DMAP) (1 equiv) were added to a solution of **5** (1 equiv) and the benzothiazole derivative **6** (1 equiv) in DCM (25 mL), and the mixture was left stirred for 24 h at room temperature under nitrogen. The solvent was removed in vacuo and the residue was purified by column chromatography on silica gel eluted with dichloromethane:methanol (6:1) to give the title compounds.

4.1.5.1. N-(4-(Benzo[*d*]thiazol-2-yl)phenyl)-6-(1,2,3,4-tetrahydroacridin-9-ylamino)hexanamide (7a).

Compounds **5** and **6a** afforded the title compound as light yellow crystals. Yield: 40%; mp 154–155 °C; ^{1}H NMR (300 MHz, CDCl$_3$) δ: 9.46 (br s, N*H*), 8.28 (d, *J* = 8.2 Hz, 1H, Ar*H*), 8.14 (d, *J* = 8.6 Hz, 1*H*, Ar*H*), 7.99 (d, *J* = 8.2 Hz, 1H, Ar*H*), 7.92–7.85 (m, 4H, Ar*H*), 7.55 (t, *J* = 7.3 Hz, 1H, Ar*H*), 7.48–7.44 (m, 1H, Ar*H*), 7.37–7.29 (m, 2H, Ar*H*), 6.76–6.67 (m, 1H, Ar*H*), 3.87 (t, *J* = 6.9 Hz, 2H, C*H*$_2$), 3.17 (t, *J* = 6.0 Hz, 2H, C*H*$_2$), 2.57 (t, *J* = 6.0 Hz, 2H, C*H*$_2$), 2.51 (t, *J* = 6.9 Hz, 2H, C*H*$_2$), 1.91–1.73 (m, 8H (CH$_2$)$_4$), 1.53 (t, *J* = 6.9 Hz, 2H, C*H*$_2$); ^{13}C NMR (400 MHz, CDCl$_3$) δ: 174.5 (C=O), 169.4, 157.0, 155.0, 154.4, 147.3, 145.7, 142.9, 135.9, 130.9, 129.8 (2 carbons), 129.1, 127.6, 126.4, 125.8, 125.1, 142.9, 123.5, 122.8, 120.9, 120.1, 115.7 (22 aromatic C), 38.2 (*N*-CH$_2$ aliphatic chain), 37.7, 32.8, 31.7, 27.4, 26.2, 25.7, 23.7, 23.1 (8 aliphatic C); MS 521 (M$^+$), 522 (M+1)$^+$. Anal. (C$_{32}$H$_{32}$N$_4$OS·0.33H$_2$O·8.65CH$_3$CN) C, H, N, S.

4.1.5.2. N-(4-(Benzo[*d*]thiazol-2-ylmethyl)phenyl)-6-(1,2,3,4-tetrahydroacridin-9-ylamino)hexanamide (7b).

Compounds **5** and **6b** afforded the title compound as light yellow crystals. Yield: 42%; mp 104–105 °C; ^{1}H NMR (300 MHz, CDCl$_3$) δ: 9.79 (br s, N*H*), 8.20 (d, *J* = 8.5 Hz, 1H, Ar*H*), 8.15 (d, *J* = 8.7 Hz, 1H, Ar*H*), 7.88 (d, *J* = 8.1 Hz, 1H, Ar*H*), 7.74–7.69 (m, 3H, Ar*H*), 7.50 (t, *J* = 7.6 Hz, 1H, Ar*H*), 7.39–7.35 (m, 1H, Ar*H*), 7.29–7.24 (m, 2H, Ar*H*), 7.15 (d, *J* = 8.4 Hz, 2H, Ar*H*), 6.62 (br s, N*H*), 4.28 (s, 2H, C*H*$_2$-S), 3.81 (s, 2H, C*H*$_2$), 3.03 (s, 2H, C*H*$_2$), 2.55–2.50 (m, 4H, C*H*$_2$-C*H*$_2$), 1.84 (t, *J* = 7.0 Hz, 2H, C*H*$_2$), 1.73 (t, *J* = 7.0 Hz, 2H, C*H*$_2$), 1.67 (br s, 4H, C*H*$_2$-C*H*$_2$), 1.42 (t, *J* = 7.0 Hz, 2H, C*H*$_2$); ^{13}C NMR (400 MHz, CDCl$_3$) δ: 172.4 (C=O), 171.7, 155.7, 153.2, 151.0, 139.1, 138.4, 135.6, 132.3, 132.2, 129.5 (2 carbons), 126.6, 125.1, 125.0, 124.8, 122.7, 121.7, 120.5, 120.4 (2 carbons), 116.1, 111.5 (22 aromatic C), 64.1 (*N*-CH$_2$ aliphatic chain), 50.6, 48.0, 40.12, 36.5, 29.9, 28.8, 25.6, 24.7, 22.0, (9 aliphatic C); *m/z*: 535 (M$^+$), 536 (M+1)$^+$; Anal. (C$_{33}$H$_{34}$N$_4$OS·2.6EtOH) C, H, N, S.

4.1.5.3. N-(4-(Benzo[*d*]thiazol-2-yl)benzyl)-6-(1,2,3,4-tetrahydroacridin-9-ylamino)hexanamide (7c).

Compounds **5** and **6c** afforded the title compound as colorless crystals. Yield: 38%; mp 192–193 °C; ^{1}H NMR (300 MHz, CDCl$_3$) δ: 8.20 (d, *J* = 8.4 Hz, 1H, Ar*H*), 8.13 (d, *J* = 8.6 Hz, 1H, Ar*H*), 7.96 (d, *J* = 8.0 Hz, 1H, Ar*H*), 7.84–7.77 (m, 4H, Ar*H*), 7.53 (t, *J* = 7.6 Hz, 1H, Ar*H*), 7.44 (t, *J* = 7.1 Hz, 1H, Ar*H*), 7.37–7.30 (m, 3H, Ar*H*), 4.45 (s, 2H, C*H*$_2$-N), 3.71 (t, *J* = 6.8 Hz, 2H, C*H*$_2$), 3.03 (t, *J* = 6.0 Hz, 2H, C*H*$_2$), 2.51 (t, *J* = 5.8 Hz, 2H, C*H*$_2$), 2.38 (t, *J* = 7.0 Hz, 2H, C*H*$_2$), 1.76–1.67 (m, 8H, (CH$_2$)$_4$), 1.40 (t, *J* = 7.1 Hz, 2H, C*H*$_2$); ^{13}C NMR (400 MHz, CDCl$_3$),

δ: 173.6 (C=O), 167.6, 155.1, 154.1, 151.4, 142.3, 139.4, 134.9, 132.3, 131.9, 128.3, 127.5 (2 C), 126.6 (2 C), 125.4, 125.0, 124.5, 123.1, 121.7, 121.0, 116.1, 112.3 (22 aromatic C), 64.0 (N-CH$_2$ aliphatic chain), 48.0, 43.0, 35.7, 30.2, 28.9, 25.8, 24.9, 22.05, 20.85 (9 aliphatic C); MS: 535 (M$^+$), 536 (M+1)$^+$. Anal. (C$_{33}$H$_{34}$N$_4$OS·1.8EtOH) C, H, N, S.

4.1.5.4. N-(3-(Benzo[*d*]thiazol-2-yl)propyl)-6-(1,2,3,4-tetrahydroacridin-9-ylamino)hexanamide (7d).

Compounds **5** and **6d** afforded the title compound as colorless crystals. Yield: 35%; mp 94–95 °C; ^{1}H NMR (300 MHz, CDCl$_3$) δ: 8.34 (d, *J* = 8.0 Hz, 1H, Ar*H*), 8.17 (d, *J* = 8.6 Hz, 1H, Ar*H*), 7.87 (d, *J* = 8.0 Hz, 1H, Ar*H*), 7.77 (d, *J* = 7.2 Hz, 1H, Ar*H*), 7.55 (t, *J* = 7.3 Hz, 1H, Ar*H*), 7.42–7.29 (m, 3H, Ar*H*), 6.99 (br s, 1H, N*H*), 3.86 (t, *J* = 7.0 Hz, 2H, C*H*$_2$), 3.39 (t, *J* = 6.5 Hz, 2H, C*H*$_2$), 3.18–3.14 (m, 4*H*, C*H*$_2$-C*H*$_2$), 2.61 (t, *J* = 6.0 Hz, 2H, C*H*$_2$), 2.27 (t, *J* = 7.1 Hz, 2H, C*H*$_2$), 2.11 (t, *J* = 7.1 Hz, 2H, C*H*$_2$), 1.88–1.76 (m, 6H, (CH$_2$)$_3$), 1.70 (t, *J* = 7.4 Hz, 2H, C*H*$_2$), 1.46 (t, *J* = 7.2 Hz, 2H, C*H*$_2$); ^{13}C NMR (400 MHz, CDCl$_3$), δ: 173.1 (C=O), 171.4, 155.0, 153.16, 135.2, 131.9, 126.8 (2 C), 125.1, 125.1, 124.2, 122.9, 121.7 (2 carbons), 116.4, 111.5, 109.2 (16 aromatic C), 63.9 (N-CH$_2$ aliphatic chain), 48.3, 38.9, 35.9, 31.9, 30.5, 29.8, 29.1, 26.0, 24.8, 24.0, 22.1, 21.0 (11 aliphatic C); MS: 487 (M$^+$), 488 (M+1)$^+$. Anal. (C$_{29}$H$_{34}$N$_4$OS·2.54H$_2$O·6.33CH$_3$CN) C, H, N, S.

4.1.5.5. N-(5-(Benzo[*d*]thiazol-2-yl)pentyl)-6-(1,2,3,4-tetrahydroacridin-9-ylamino)hexanamide (7e).

Compounds **5** and **6e** afforded the title compound as colorless crystals. Yield: 44%; mp 78–79 °C; ^{1}H NMR (300 MHz, CDCl$_3$) δ: 8.36 (d, *J* = 8.5 Hz, 1H, Ar*H*), 8.17 (d, *J* = 8.6 Hz, 1H, Ar*H*), 7.91 (d, *J* = 8.0 Hz, 1H, Ar*H*), 7.80 (d, *J* = 7.7 Hz, 1H, Ar*H*), 7.61 (t, *J* = 7.6 Hz, 1H, Ar*H*), 7.45–7.30 (m, 3H, Ar*H*), 6.37 (br s, 1H, N*H*), 3.86 (t, *J* = 7.0 Hz, 2H, C*H*$_2$), 3.28–3.18 (m, 4H, (CH$_2$)$_2$), 3.08 (t, *J* = 7.5 Hz, 2H, C*H*$_2$), 2.63 (t, *J* = 5.8 Hz, 2H, C*H*$_2$), 2.24 (t, *J* = 7.0 Hz, 2H, C*H*$_2$), 1.90–1.82 (m, 8H, (CH$_2$)$_4$), 1.70 (t, *J* = 7.3 Hz, 2H, C*H*$_2$), 1.58 (t, *J* = 7.2 Hz, 2H, C*H*$_2$), 1.49–1.40 (m, 4H, (CH$_2$)$_2$); ^{13}C NMR (400 MHz, CDCl$_3$) δ: 173.0 (C=O), 172.0, 155.1, 153.3, 152.1, 135.2, 131.9, 126.0 (2 carbons), 125.0, 124.9, 124.3, 122.5, 121.7 (2 carbons), 116.5, 111.6 (16 aromatic C), 64.0 (N-CH$_2$ aliphatic chain), 48.3, 39.3, 35.9, 34.2, 30.4, 29.4, 29.3, 26.5, 25.9, 24.8, 24.1 22.2, 21.0 (13 aliphatic C); MS: 515 (M$^+$), 516 (M+1)$^+$. Anal. (C$_{31}$H$_{38}$N$_4$OS·2.02H$_2$O·2.31CH$_3$CN); Anal. (C$_{31}$H$_{38}$N$_4$OS·2.02 H$_2$O·2.31CH$_3$CN) C, H, N, S.

4.2. Acetylcholinesterase inhibition

The determination of the AChE inhibitory capacity of the synthesized compounds was performed by an adaptation of a method previously described.[30] The buffer solution used in this enzymatic assay was 2-[4-(2-hydroxyethyl)-1-piperazine]ethanesulfonic acid (HEPES) at 50 mM and pH 8. The Ellman reagent, 5,5′-dithiobis-(2-nitrobenzoic acid) (DTNB, 3 mM) was diluted in a HEPES buffer solution containing NaCl (50 mM) and MgCl$_2$ (20 mM). Acetylcholinesterase stock solution was prepared by dissolving 500 U (extracted from *electrophorus electricus* and purchased from Sigma–Aldrich) in TRIS buffer (50 mM, pH 8) (10 mL). The enzyme was later diluted with HEPES buffer to give the final AChE concentration conditions, 1.75 U mL^{-1}. A 16 mM aqueous solution of the enzyme substrate, acetylcholine iodide (AChI), was also prepared. Stock solutions of the tested compounds were prepared in methanol (1 mg/mL), due to their hydrophobic nature, and five different concentrations were used in order to obtain AChE inhibition ranging between 20% and 90%.

The final assay solution resulted from assembling several solutions: 374 µL of HEPES (50 mM, pH 8), 476 µL of DTNB; a variable

volume (10, 20, 30, 40, 50 μL) of inhibitor solution, 25 μL of the AChE solution and the necessary amount of methanol to attain 0.925 mL of sample mixture in a 1 mL cuvette. The samples were left to incubate for 15 min. Subsequently, 75 μL of substrate solution was added. The initial rate of the enzymatic reaction was monitored by reading the solution absorbance at 405 nm, recorded on a Perkin-Elmer Lambda 35 UV–Vis spectrophotometer, during the first 5 min of the reaction time. Assays were also run with a blank solution containing all the components except the AChE solution (that was replaced by buffer HEPES), to account for the non-enzymatic reactions. The velocities of the reaction were calculated, as well as the enzyme activity. A control reaction was carried out using the sample solvent (methanol) in the absence of any tested compound and it was considered as 100% activity. Each concentration was analyzed in quintuplicate. The percent inhibition of the enzyme activity due to the presence of increasing test compound concentration was calculated by the following Eq. (1),

$$\%I = 100 - \left(\frac{v_I}{v_0} \times 100 \right) \tag{1}$$

in which v_I is the initial reaction rate in the presence of inhibitor, and v_0 is the initial rate of the control reaction. The inhibition curves were obtained by plotting the percentage of enzymatic inhibition versus inhibitor concentration and a calibration curve was drawn from which the linear regression parameters were obtained. Data presented are the average of three independent experiments ± SD.

4.3. Inhibition of self-mediated Aβ$_{42}$ aggregation

Amyloid β-peptide (1–42) (Aβ$_{42}$), was purchased from Aldrich as a lyophilized powder and stored at −20 °C. The samples were treated with 1,1,1,1,1,1-hexafluoropropan-2-ol (HFIP) to avoid self-aggregation and reserved. HFIP pre-treated Aβ$_{42}$ samples were re-solubilized with a CH_3CN/Na$_2CO_3$ (300 μM)/NaOH (250 μM) (48.3:48.3:4.3, v/v/v) solvent mixture in order to have a stable stock solution. This Aβ$_{42}$ alkaline solution (500 μM) was diluted in phosphate buffer (0.215 M, pH 8.0) to obtain a 20 μM solution. Compounds under study were firstly dissolved in methanol (1 mg/mL) due to their hydrophobic nature, and then further diluted in phosphate buffer to a final concentration of 50 μM.

To study the Aβ$_{42}$ aggregation inhibition, a reported method, based on the fluorescence emission of thioflavin T (ThT), was followed.[39,40] Firstly, Aβ$_{42}$ (10 μL) samples and the tested compounds (10 μL) were diluted with the phosphate buffer to a final concentration of 20 μM (Aβ) and 50 μM (compounds), and then were incubated for 24 h at 37 °C, without stirring. As for the control, a sample of the peptide was incubated under identical conditions but without the inhibitor. After incubation, the samples were added to a black, flat-, and clear bottom 96-well plate (BD Falcon) with 180 μL of 1.5 μM ThT in 50 mM glycine–NaOH (pH 8.5). Blank samples were prepared for each concentration in a similar way, devoid of peptide. After 5 min incubation with the dye, the ThT fluorescence was measured using a Spectramax Gemini EM (molecular Devices) at the following wavelengths: excitation (446 nm) and emission (490 nm). The percent inhibition of the self-induced aggregation due to the presence of the test compound was calculated on basis of Eq. (2), in which IF_i and IF_0 correspond to the fluorescence

$$I\% = 100 - \left(\frac{IF_i}{IF_0} \times 100 \right) \tag{2}$$

intensities, in the presence and absence of the test compound, respectively, minus the fluorescence intensities due to the respective blanks. The reported values were obtained as the mean ± SEM of duplicate of two different experiments.

4.4. Antioxidant activity

The antioxidant activity was evaluated by the DPPH method previously described.[44] To a 2.5 mL solution of DPPH (0.002%) in methanol, four samples of each compound solution were added with different volumes to obtain different concentrations of the tested compound. The volume required for the final total volume (3.5 mL) was attained with methanol. The samples were incubated for 30 min at room temperature. The absorbance was measured at 517 nm against the corresponding blank (methanol). The antioxidant activity was calculated by Eq. (3),[34]

$$\%AA = \frac{A_{DPPH} - A_{sample}}{A_{DPPH}} \tag{3}$$

in which AA is the antioxidant activity, A_{DPPH} is the absorbance of the DPPH solution against the blank, A_{sample} is the absorbance of the sample compound against the blank. The tests were carried out in triplicate. The compound concentrations providing 50% of antioxidant activity (EC$_{50}$) were obtained by plotting the antioxidant activity against the compound concentration.

4.5. Human subjects and creation of cybrid cell lines

Subject participation was approved by the Kansas University Medical Center's Institutional Review Board. Subjects for this study were recruited from the University of Kansas Alzheimer's Disease Center (KU ADC). Each subject was determined, based on cognitive testing and by a memory disorders subspecialist clinician, to meet criteria for normal cognition (control status), mild cognitive impairment (MCI), or sporadic Alzheimer's disease (AD). After providing informed consent, sporadic AD ($n = 8$), MCI ($n = 7$) and age-matched control ($n = 7$) subjects underwent a 10 mL phlebotomy using tubes containing acid–citrate–dextrose as an anticoagulant. The age of the AD subject platelet donors was 71.5 ± 9.7 years, the age of the MCI platelet donors was 72.3 ± 6.6, and the age of the control subject platelet donors was 73.9 ± 7.7.

Cybrid cell lines were created on an SHSY-5Y cell nuclear background. To generate the cybrid lines used in these studies, platelets from human subjects were mixed with SHSY-5Y cells previously depleted of endogenous mtDNA (ρ0 cells). During the overall cybrid generation procedure several different types of media were used. For each medium, Dulbecco's modified Eagle's medium (DMEM) medium was obtained from Gibco-Invitrogen, while non-dialyzed or dialyzed fetal bovine serum (FBS) was obtained from Sigma. SHSY-5Y ρ0 cell growth medium consisted of DMEM supplemented with 10% non-dialyzed FBS, 200 μg/mL sodium pyruvate, 150 μg/mL uridine, and 1% penicillin–streptomycin solution. SHSY-5Y cybrid selection medium consisted of DMEM supplemented with 10% dialyzed FBS and 1% penicillin–streptomycin solution. The selection process lasted 6 weeks. After cell line selection was completed, each line, including SHSY-5Y was continuously maintained in a cybrid growth medium containing DMEM supplemented with 10% non-dialyzed FBS and 1% penicillin–streptomycin solution for over 2 months prior to biochemical and molecular assays.

4.6. Cell treatments and viability

The tested compounds (**7a–7e**) were dissolved in DMSO at a concentration of 10 mM and aliquots were stored at −20 °C. These compounds were added to the medium at 2.5 μM final concentration. Before the addition of Aβ$_{42}$, cells were pre-incubated for 3 h with tacrine–BTA hybrids compounds. The final concentration of DMSO in culture media did not exceed 0.05% (v/v) and no alterations on cells were observed. For all conditions tested, control

4568

R. S. Keri et al. / Bioorg. Med. Chem. 21 (2013) 4559–4569

experiments were performed in which the compounds tested or $A\beta_{42}$ were not added.

Cell reduction ability as a surrogate of cell viability was measured by using a quantitative colorimetric assay with MTT according to the method of Mosmann (1983).[30,50] In brief, cells were incubated with MTT solution (in sodium medium) for 3 h at 37 °C. The medium was then discarded, the cells were dissolved with isopropanol/HCl, and thereafter the absorbance at 570 nm was measured using a Spectramax Plus 384 spectrophotometer (Molecular Devices). MTT reduction ability was expressed as a percentage of the control value obtained for untreated cells.

4.7. Molecular modeling

To perform our docking studies the X-ray crystallographic structure of *Torpedo californica*-AChE (TcAChE) complexed with an inhibitor was taken from RCSB Protein Data Bank (PDB entry 1ODC), in order to be used as receptor. This structure was chosen because of the similarity between its original inhibitor (*N*-quinolin-4-yl-*N*′-(1,2,3,4-tetrahydroacridin-9-yl)octane-1,8-diamine) and our ligands: all have a tacrine moiety and an aromatic group linked through an alkyl chain.[51] The original structure was treated using Maestro v. 9.3,[52] by removing the original ligand, solvent, and co-crystallization molecules, and then adding the hydrogen atoms. The ligands were built using Maestro, and then, using Ghemical v. 2.0,[53] they were submitted to random conformational search (RCS) of 1000 cycles, and 2500 optimization steps using Tripos 5.2 force field.[54]

The minimized ligands were docked into the AChE structure with GOLD software v. 5.1,[32] and the zone of interest was defined as the residues within 10 Å from the original position of the ligand in the crystal structure. The 'allow early termination' option was deactivated, and the remaining default parameters of Gold were used. The ligands were subjected to 100 genetic algorithm steps using ASP as fitness function.

4.8. Prediction of pharmacokinetic proprieties

To analyze the potential of the new compounds as new anti-AD drugs, a brief prediction on pharmacokinetic proprieties was performed in silico. Parameters such as the lipo-hydrophilic character ($c \log P$), blood–brain barrier partition coefficient ($\log BB$), the ability to be absorbed through the intestinal tract (Caco-2 cell permeability) and CNS activity were calculated.

The ligands were built and minimized as previously mentioned for the docking studies. The structures were submitted to the calculation of these relevant pharmacokinetic proprieties and descriptors using QikProp v. 2.5.[45] These predictions are for orally delivered drugs and assume nonactive transport.

Acknowledgments

Supplementary data

Supplementary data associated with this article can be found, in the online version, at http://dx.doi.org/10.1016/j.bmc.2013.05.028.

References and notes

1. Holden, M.; Kelly, C. *Adv. Psychiatr. Treat.* **2002**, *8*, 89.
2. Alzheimer's Disease International, World Alzheimer report 2011, p. 1.
3. Terry, A. V., Jr.; Buccafusco, J. J. *J. Pharmacol. Exp. Ther.* **2003**, *306*, 821.
4. Bartus, R. T. *Exp. Neurol.* **2000**, *163*, 495.
5. Buée, L.; Bussière, T.; Buée-Scherrer, V.; Delacourte, A.; Hof, P. R. *Brain Res. Rev.* **2000**, *33*, 95.
6. Tolnay, M.; Probst, A. *Neuropathol. Appl. Neurobiol.* **1999**, *25*, 171.
7. Hardy, J.; Selkoe, D. J. *Science* **2002**, *297*, 353.
8. LaFeria, L. M.; Green, K. N.; Oddo, S. *Nat. Rev. Neurosci.* **2007**, *8*, 499.
9. Rogers, S. L.; Farlow, M. R.; Doody, R. S.; Mohs, R.; Friedhoff, L. T. *Neurology* **1998**, *50*, 136.
10. Cummings, J. L. *Am. J. Psychiat.* **2000**, *157*, 4.
11. Giacobini, E. *Neurochem. Int.* **1998**, *32*, 413.
12. Summers, W. K.; Majovski, L. V.; Marsh, G. M.; Tachiki, K.; Kling, A. N. *Engl. J. Med.* **1986**, *315*, 1241.
13. Tumiatti, V.; Minarini, A.; Bolognesi, M. L.; Milelli, A.; Rosini, M.; Melchiorre, C. *Curr. Med. Chem.* **1825**, *2010*, 17.
14. Romero, A.; Cacabelos, R.; Oset-Gasque, M. J.; Samadi, A.; Marco-Contelles, J. *Bioorg. Med. Chem. Lett.* **1916**, *2013*, 23.
15. Fernández-Bachiller, M. I.; Pérez, C.; González-Muñoz, G. C.; Conde, S.; López, M. G.; Villarroya, M.; García, A. G.; Rodríguez-Franco, M. I. *J. Med. Chem.* **2010**, *53*, 4927.
16. Wang, Y.; Guan, X. L.; Wu, P. F.; Wang, C. M.; Cao, H.; Li, L.; Guo, X. J.; Wang, F.; Xie, N.; Jiang, F. C.; Chen, J. G. *J. Med. Chem.* **2012**, *55*, 3588.
17. Szymanski, P.; Karpiński, A.; Mikiciuk-Olasik, E. *Eur. J. Med. Chem.* **2011**, *46*, 3250.
18. (a) Luo, W.; Li, Y. P.; He, Y.; Huang, S. L.; Li, D.; Gu, L. Q.; Huang, Z. S. *Eur. J. Med. Chem.* **2011**, *46*, 2609; (b) Luo, W.; Li, Y. P.; He, Y.; Huang, S. L.; Tan, J. H.; Ou, T. M.; Li, D.; Gu, L. Q.; Huang, Z. S. *Bioorg. Med. Chem.* **2011**, *19*, 763.
19. Roberson, E. D.; Scearce-Levie, K.; Palop, J. J.; Yan, F.; Cheng, I. H.; Wu, T.; Gerstein, H.; Yu, G. Q.; Mucke, L. *Science* **2007**, *316*, 750.
20. Khlistunova, I.; Biernat, J.; Wang, Y. P.; Pickhardt, M.; von Bergen, M.; Gazova, Z.; Mandelkow, E.; Mandelkow, E. M. *J. Biol. Chem.* **2005**, *281*, 1205.
21. Belluti, F.; Rampa, A.; Gobbi, S.; Bisi, A. A patent review (2010–2012), Expert Opin. Ther. Pat. 02/2013.
22. Jakob-Roetne, R.; Jacobsen, H. *Angew. Chem., Int. Ed.* **2009**, *48*, 3030.
23. Yona, R. L.; Mazères, S.; Faller, P.; Gras, E. *ChemMedChem* **2008**, *3*, 63.
24. Alagille, D.; DaCosta, H.; Baldwin, R. M.; Tamagnan, G. D. *Bioorg. Med. Chem. Lett.* **2011**, *21*, 2966.
25. Soto-Ortega, D. D.; Murphy, B. P.; Gonzalez-Velasquez, F. J.; Wilson, K. A.; Xie, F.; Wang, Q.; Moss, M. A. *Bioorg. Med. Chem.* **2011**, *19*, 2596.
26. Choi, M. M.; Kim, E. A.; Hahn, H. G.; Dal Nam, K.; Yang, S. J.; Choi, S. Y.; Kim, T. U.; Cho, S. W.; Huh, J. W. *Toxicology* **2007**, *239*, 156.
27. Rosini, M.; Simoni, E.; Bartolini, M.; Cavalli, A.; Ceccarini, L.; Pascu, N.; McClymont, D. W.; Tarozzi, A.; Bolognesi, M. L.; Minarini, A.; Tumiatti, V.; Andrisano, V.; Mellor, I. R.; Melchiorre, C. *J. Med. Chem.* **2008**, *51*, 4381.
28. Huang, L.; Su, T.; Shan, W.; Luo, Z.; Sun, Y.; He, F.; Li, X. *Bioorg. Med. Chem.* **2012**, *20*, 3038.
29. Martins, C.; Carreiras, M. C.; Leon, R.; de los Rios, C.; Bartolini, M.; Andrisano, V.; Iriepa, I.; Moraleda, I.; Galvez, E.; Garcia, M.; Egea, J.; Samadi, A.; Chioua, M.; Marco-Contelles, J. *Eur. J. Med. Chem.* **2011**, *46*, 6119.
30. Nunes, A.; Marques, S. M.; Quintanova, C.; Silva, D. F.; Cardoso, S. M.; Chaves, S.; Santos, M. A. *Dalton Trans.* **2013**, *42*, 6058.
31. Ansari, M. A.; Scheff, S. W. *J. Neuropathol. Exp. Neurol.* **2010**, *69*, 155.
32. Jones, G.; Willett, P.; Glen, R. C.; Leach, A. R.; Taylor, R. *J. Mol. Biol.* **1997**, *267*, 727.
33. Protein Data Base (PDB). http://www.pdb.org/pdb/home/home.do (accessed October 2012–February 2013).
34. Sebestík, J.; Marques, S. M.; Falé, P. L.; Santos, S.; Arduíno, D. M.; Cardoso, S. M.; Oliveira, C. R.; Serralheiro, M. L.; Santos, M. A. *J. Enzyme Inhib. Med. Chem.* **2011**, *26*, 485.
35. Inestrosa, N. C.; Alvarez, A.; Pérez, C. A.; Moreno, R. D.; Vincente, M.; Linker, C.; Casanueva, O. I.; Soto, C.; Garrido, J. *Neuron* **1996**, *16*, 881.
36. Bartolini, M.; Bertucci, C.; Cavrini, V.; Andrisano, V. *Biochem. Pharm.* **2003**, *65*, 407.
37. Sargent, L. J.; Small, L. *J. Org. Chem.* **1946**, *11*, 359.
38. Hu, M. K.; Lu, C. F. *Tetrahedron Lett.* **1815**, *2000*, 41.
39. Bartolini, M.; Bertucci, C.; Bolognesi, M. L.; Cavalli, A.; Melchiorre, C.; Andrisano, V. *ChemBioChem* **2007**, *8*, 2152.
40. Chao, X.; He, X.; Yang, Y.; Zhou, X.; Jin, M.; Liu, S.; Cheng, Z.; Liu, P.; Wang, Y.; Yu, J.; Tan, Y.; Huang, Y.; Qin, J.; Rapposelli, S. *Bioorg. Med. Chem. Lett.* **2012**, *22*, 6498.
41. Hawe, A.; Sutter, M.; Jiskoot, W. *Pharm. Res.* **2007**, *25*, 1487.
42. Silva, D. F.; Santana, I.; Esteves, A. R.; Baldeiras, I.; Arduino, D. M.; Oliveira, C. R.; Cardoso, S. M. *Curr. Alzheimer Res.* **2013**, *10*, 180.
43. DeKosky, S. T.; Marek, K. *Science* **2003**, *302*, 830.

44. Tepe, B.; Daferera, D.; Sokmen, A.; Sokmen, M.; Polissiou, M. *J. Agric. Food Chem.* **2005**, *90*, 333.
45. QikProp, version 2.5, Schrödinger, LLC, New York, NY, 2005.
46. Lipinski, C. A.; Lombardo, F.; Dominy, B. W.; Feeney, P. *J. Adv. Drug Deliv. Rev.* **1997**, *23*, 3.
47. Armarego, W. L. F.; Perrin, D. D. *Purification of Laboratory Chemicals*, 4th ed.; Butterworth-Heinemann: Oxford, 1999.
48. Camps, P.; Formosa, X.; Munoz-Torrero, D.; Petrignet, J.; Badia, A.; Clos, M. V. *J. Med. Chem.* **2005**, *48*, 1701.
49. Shi, D. F.; Bradshaw, T. D.; Wrigley, S.; McCall, C. J.; Lelieveld, P.; Fichtner, I.; Stevens, M. F. *J. Med. Chem.* **1996**, *39*, 3375.
50. Mosmann, T. *J. Immunol. Methods* **1983**, *65*, 55.
51. Rydberg, E. H.; Brumshtein, B.; Greenblatt, H. M.; Wong, D. M.; Shaya, D.; Williams, L. D.; Carlier, P. R.; Pang, Y.; Silman, I.; Sussman, J. L. *J. Med. Chem.* **2006**, *49*, 5491.
52. Maestro, version 9.3. Schrödinger Inc.: Portland, OR, 2012.
53. Hassinen, T.; Peräkylä, M. *J. Comput. Chem.* **2001**, *22*, 1229.
54. Clark, M.; Cramer, R. D., III; Van Opdenbosch, N. *J. Comput. Chem.* **2004**, *10*, 982.